Growth rate and surfactant-assisted enhancements of rare-earth arsenide InGaAs nanocomposites for terahertz generation

R. Salas, S. Guchhait, S. D. Sifferman, K. M. McNicholas, V. D. Dasika, D. Jung, E. M. Krivoy, M. L. Lee, and S. R. Bank

Citation: APL Materials **5**, 096106 (2017); doi: 10.1063/1.4991589
View online: http://dx.doi.org/10.1063/1.4991589
View Table of Contents: http://aip.scitation.org/toc/apm/5/9
Published by the American Institute of Physics

Growth rate and surfactant-assisted enhancements of rare-earth arsenide InGaAs nanocomposites for terahertz generation

R. Salas,[1] S. Guchhait,[1] S. D. Sifferman,[1] K. M. McNicholas,[1] V. D. Dasika,[1] D. Jung,[2] E. M. Krivoy,[1] M. L. Lee,[3] and S. R. Bank[1]
[1]*Microelectronics Research Center, The University of Texas at Austin, Austin, Texas 78758, USA*
[2]*The Institute for Energy Efficiency, University of California, Santa Barbara, Santa Barbara, California 93106, USA*
[3]*Department of Electrical and Computer Engineering, University of Illinois, Urbana, Illinois 61801, USA*

(Received 22 June 2017; accepted 1 September 2017; published online 25 September 2017)

We report the effects of the growth rate on the properties of III-V nanocomposites containing rare-earth-monopnictide nanoparticles. In particular, the beneficial effects of surfactant-assisted growth of LuAs:$In_{0.53}Ga_{0.47}As$ nanocomposites were found to be most profound at reduced LuAs growth rates. Substantial enhancement in the electrical and optical properties that are beneficial for ultrafast photoconductors was observed and is attributed to the higher structural quality of the InGaAs matrix in this new growth regime. The combined enhancements enabled a >50% increase in the amount of LuAs that could be grown without degrading the quality of the InGaAs overgrowth. Dark resistivity increased by ~25× while maintaining carrier mobilities over 3000 cm^2/V s; carrier lifetimes were reduced by >2×, even at high depositions of LuAs. The combined growth rate and surfactant enhancements offer a previously unexplored regime to enable high-performance fast photoconductors that may be integrated with telecom components for compact, broadly tunable, heterodyne THz source and detectors. https://doi.org/10.1063/1.4991589

Compact, tunable, room-temperature, continuous-wave terahertz (THz) sources are attractive for numerous potential applications.[1–5] While continued efforts to increase output powers beyond the microwatt range have resulted in considerable progress in optical and RF solid state THz emitters,[6–11] these devices remain limited by low output powers and uncertainty in the frequency tunability. One promising path of development is photomixer technology, which offers a path toward tunable continuous-wave THz generation from a single compact device.[12,13] Photomixers operate by modulating an induced current at THz frequencies through the interference of two continuous-wave single frequency lasers incident on a photoconductive material. The photogenerated current is subsequently coupled to a planar antenna and emitted as THz radiation.[14,15] Candidate photoconductive materials are characterized by high resistivities, high carrier mobilities, and short carrier lifetimes.[16]

Previous and current photoconductive materials work has focused mainly on low-temperature-grown (LTG) GaAs,[17] superlattices of epitaxially embedded ErAs[18–20] and LuAs[21–23] nanoparticles in GaAs, and co-deposited nanoparticles of ErAs in a dilute-bismide matrix of GaAsBi.[24] The recent ErAs:GaAsBi approach reported by Bomberger *et al.* is a noteworthy advance as these materials exhibited excellent dark resistivity and can be pumped with longer-wavelength sources, though more work is needed to achieve high carrier mobilities at the low growth temperatures that are required for dilute-bismide growth. Development of fast photoconductive materials with smaller bandgaps, such as $In_{0.53}Ga_{0.47}As$, would take advantage of the mature telecommunications component infrastructure available at 1550 nm.[25,26] Despite considerable efforts with small bandgap materials using InP-based

nipnip[27,28] and uni-traveling carrier[29,30] diodes, plasmonic enhancements,[31,32] and promising materials such as LTG-InGaAs[33] and LTG-InGaAs/InAlAs multilayer heterostructures,[34] devices based on such materials have yet to yield output powers beyond the microwatt range at THz frequencies. Nanocomposites based on rare-earth arsenide (RE-As) nanoparticle superlattice[35–37] and codeposited[38–40] structures in an InGaAs matrix have also been investigated but were found to exhibit prohibitively low dark resistivities. Our previous studies of superlattices containing different RE-As species suggested that the quality of the matrix overgrowth could have a considerable impact on nanocomposite properties.[37] Aside from previous studies into various growth temperatures in GaAs-based nanocomposites,[41] there has been little research exploring nanoparticle morphology as a means to improve the structural quality of the matrix in superlattices and its effects on the photoconductive properties. Moreover, the role of the RE-V growth rate has been only scarcely studied and yielded mixed results.[42,43]

The effect on nanoparticle morphology due to different RE-As growth rates was first explored in the ErSb:GaSb system.[42] The resulting nanocomposites showed a modest decrease in the carrier lifetime as the ErSb growth rate was decreased from 0.09 ML/s to 0.04 ML/s; however, the effects on the electrical properties were less advantageous as the resistivity decreased while mobility improved only slightly.[43] The nanoparticle size and density were, however, affected significantly by the ErSb growth rate. Specifically, lower ErSb growth rates resulted in a lower density of larger nanoparticles. The effects of RE-As growth rate on the structural quality of the matrix overgrowth in superlattices and its effects on the properties of the nanocomposite, however, remain entirely unexplored. Here, we report the structural quality, electrical properties, and carrier lifetimes of superlattices containing LuAs nanoparticles embedded in a bismuth surfactant-enhanced InGaAs matrix,[44] grown at various LuAs growth rates. We found that, particularly when combined with surfactant-mediated growth, the RE-V growth rate has a profound effect on the nanoparticle structure and subsequent III-V overgrowth, in turn providing a path to simultaneously improve all the key properties of THz photoconductive substrates.

Superlattice samples were grown on (001)-oriented, Fe-doped, semi-insulating InP substrates by solid-source molecular beam epitaxy (MBE) in an EPI Mod Gen. II system. InGaAs layers lattice-matched to InP were grown at 490 °C and at 2.4 Å/s with an As_2/group-III beam equivalent pressure (BEP) ratio of 15 (As_2/group-III flux ratio of ~1.9) and 1×10^{-5} Torr BEP of As_2, which was held constant throughout the growth of the structures. Using separate calibration experiments similar to previous work,[45] the steady-state surface coverage of bismuth under the growth conditions used was ~12% (bismuth BEP of 1×10^{-7} Torr). This flux was applied on select samples only during growth of the InGaAs layers.[44,46] Separate high-resolution X-ray diffraction (HR-XRD) studies confirmed that the bismuth did not incorporate into InGaAs layers grown under the same conditions as the superlattices. A two second flash-off period, sufficient to desorb >99% of surface bismuth at 490 °C,[47,48] was employed prior to the growth of each RE-As nanostructure layer in all superlattices. This prevented lingering surface bismuth atoms from affecting the nanoparticle formation and/or morphology.[44] In addition, enthalpies of formation for RE-Bi compounds are ~3× less than their RE-As counterparts and are not expected to incorporate into or form nanoparticles with any remaining bismuth atoms without the incident bismuth flux while under a continuous arsenic overpressure.[49–52] Nanoparticles of LuAs with growth rates of 0.01, 0.02, and 0.07 monolayers/s (ML/s) were epitaxially embedded in a superlattice structure with depositions of LuAs repeated each period. LuAs growth rates and depositions are stated in terms of equivalent number of LuAs monolayers (MLs), as determined by reflection high energy electron diffraction (RHEED) intensity oscillations and/or HR-XRD measurements of bulk LuAs films. The superlattice structure consisted of a 150-nm InGaAs buffer layer followed by 30 periods of LuAs deposition with 40 nm of InGaAs overgrowth, similar to previous structures investigated to facilitate direct comparison.[37,44] All samples used constant LuAs depositions per period except for those used for transmission electron microscopy (TEM) studies, which varied in the amount of LuAs deposited per period. Specifically, TEM structures began with depositions of 0.2 ML in the first period and increased by 0.2 ML per period up to 3.0 ML.

Prior studies of LuAs-based nanocomposites[21,37] indicate nucleation of LuAs nanoparticles before the formation of films when grown on zincblende III-V materials, similar to other RE-V monopnictides.[53,54] The growth rate of the RE-As[42] and the amount deposited[21,55–57] affect the density

and the morphology of the nanoparticles, altering the exposed area of the III-V material between the nanoparticles available to seed the overgrowth.[58–61] As shown in Fig. 1(a), root-mean-squared (RMS) surface roughness as measured by atomic force microscopy (AFM) was over 10 nm for the superlattice grown without bismuth using 0.07 ML/s LuAs growth rate at an effective deposition of 1.6 ML. The application of bismuth as a surfactant reduced the surface roughness and delayed the onset of material degradation to higher depositions of LuAs.[44] Combining the bismuth surfactant during the InGaAs growth with a slower 0.01 ML/s LuAs growth rate further decreased the surface roughness and allowed for effective depositions up to 2.0 ML per period while maintaining an RMS surface roughness of ~1 nm. Combining these two techniques allows for a ~50% increase in the LuAs deposition in the 30-period superlattices while maintaining good structural quality, particularly as compared to the 0.07 ML/s LuAs growth rate without bismuth. HR-XRD symmetric ω-2θ scans around the (004) diffraction peak of the InP substrate [Fig. 1(a) insert] showed degraded superlattice peak fringes, indicative of poor quality period interfaces, for a LuAs growth rate of 0.07 ML/s without using bismuth surfactant. Superlattice peak fringes for the 0.07 ML/s growth rate improved significantly when bismuth was employed and improved further when the growth rate was lowered to 0.01 ML/s. Consistent with previous studies,[44] cross-sectional TEM studies with increasing deposition of LuAs nanostructures per period, shown in Fig. 1(b), indicated surface modulation after an effective LuAs deposition of 2.4 ML with progressively degraded period interfaces at higher depositions. However, by combining bismuth with a slow LuAs growth rate of 0.01 ML/s, shown in Fig. 1(c), well-defined interfaces were maintained even up to an effective deposition of 3.0 ML. Closer inspection of the 2.6 ML deposition layers of LuAs [Figs. 1(b) and 1(c) insets] show a larger nanoparticle morphology for the 0.01 ML/s compared to the 0.07 ML/s growth rate, consistent with previous investigations.[42]

This improvement in the structural quality of superlattices grown using bismuth was previously demonstrated[44] and is attributed to the altered surface kinetics of adatoms in the presence of the surfactant. However, the improvement due to the changing RE-As growth rate requires consideration. It was established[54] that a critical local density of RE atoms is required before a nanoparticle will form, since a nanoparticle with a minimum height of 4 ML is needed to stabilize the rocksalt crystal structure. Slowing the RE-As growth rate by reducing the incident RE flux means that critical local densities are less common on the surface leading to the formation of fewer nanoparticles. As RE atoms adsorb to the surface, it is more probable that the atoms will encounter an already formed nanoparticle to adhere

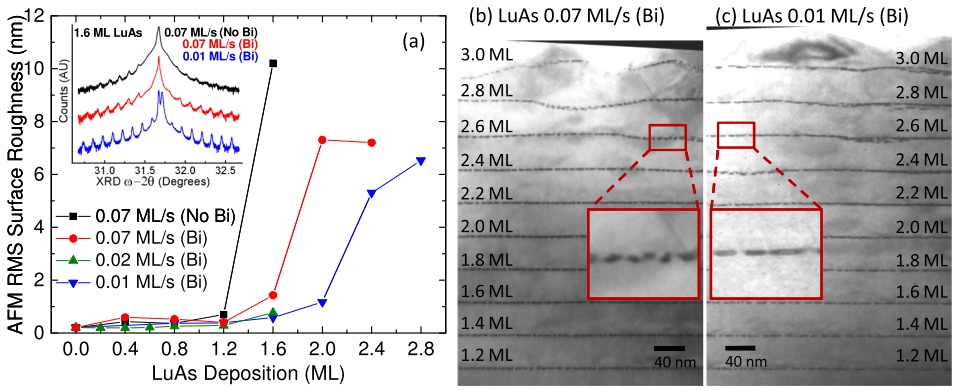

FIG. 1. (a) Root-mean-squared (RMS) surface roughness of 30-period superlattices, as measured by AFM, increases with increasing LuAs deposition, with the onset of roughening delayed by the use growth enhancements. The superlattices that combined bismuth with a slower LuAs growth rate had the lowest surface degradation at the highest depositions of LuAs. (Inset) X-ray diffraction symmetric ω-2θ scans around the (004) diffraction peak of InP for superlattices with 1.6 ML deposition of LuAs per period exhibit stronger fringe peaks, indicative of smoother and more sharply defined period interfaces, for the growth-enhanced superlattices. Cross-sectional TEM study of bismuth-enhanced LuAs-containing superlattices with increasing depositions of LuAs per period at (b) 0.07 ML/s and (c) 0.01 ML/s LuAs growth rates. The combination of bismuth and slower LuAs growth rate maintained clearly defined interfaces with minor surface modulations even at 3.0 ML of LuAs. The insets show a zoom-in view of the differences in nanoparticle morphology caused by the slower growth rate.

to, rather than reaching the critical local density with other RE atoms to form a new nanoparticle. Hence, a slower growth rate leads to fewer and larger nanoparticles, which increases the mean spacing between nanoparticles where the III-V surface is exposed. The increased III-V surface exposure allows for an improved seeding of the overgrowth, increasing the quality of the III-V overgrowth. If bismuth had also been used during the growth of the RE-As, the surface diffusion length of the RE atoms would have presumably decreased, thereby increasing the local critical density sites, and ultimately form a large number of smaller nanoparticles. As such, adding bismuth during the LuAs nanoparticle growth would negate the benefit of the slower growth rate. This interpretation is supported by the results from a 1.6 ML LuAs superlattice using a LuAs growth rate of 0.01 ML/s that used bismuth during the growth of both the InGaAs and the LuAs. This superlattice had a surface roughness twice that of an otherwise identical superlattice where bismuth was only present on the surface during the InGaAs overgrowth.

Hall measurements performed at room temperature indicated electrons as the majority carriers for all measured superlattices, consistent with previous studies of other RE-As:InGaAs nanocomposites.[26,37] The Hall measurements showed a gradual increase in dark resistivity with increasing depositions of LuAs, shown in Fig. 2(a), consistent with previous studies of RE-As:InGaAs superlattices where the RE-As nanoparticles act as recombination centers at higher depositions, reducing the mobility and conductivity.[35,37] Superlattices that combined surfactant-mediated overgrowth with a slower 0.01 ML/s LuAs growth rate showed an increase in dark resistivity to a maximum of 0.75 Ω-cm, a 70% improvement over the bismuth enhancement alone and a ~25× increase over the superlattices grown with high LuAs growth rate and without bismuth. Carrier mobilities, plotted in Fig. 2(b), decreased with increasing deposition of LuAs. However, the superlattices grown with both bismuth and 0.01 ML/s LuAs growth rate show consistently higher mobilities than other samples at their respective effective LuAs depositions; indeed, mobilities greater than 3000 cm^2/V-s were observed even at the highest deposition level studied. The increased resistivity and mobility are attributed to the improved structural quality of the InGaAs overgrowth through a reduction of the scattering and diffusion-limited transit times of the charge carriers before recombination at the nanoparticles.

Charge carrier activation energies extracted from temperature-dependent Hall measurements[35] showed a strong dependence on the effective amount of deposited RE-As. The activation energy is a reasonable proxy for the average position of the Fermi level at the RE-As/InGaAs interface throughout the superlattice as previously established.[37,44] Higher activation energies correspond to the Fermi level aligning closer to InGaAs midgap, decreasing charge carrier concentration and increasing dark resistivity. For the superlattices that combined a slow 0.01 ML/s LuAs growth rate and bismuth surfactant, the activation energies [shown in Fig. 3(a)] increased significantly over superlattices with a high LuAs growth rate with and without bismuth. This improvement is attributed to a greater

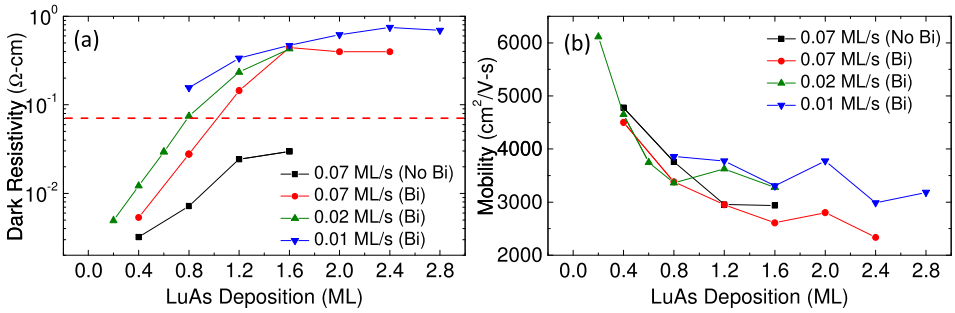

FIG. 2. Room-temperature Hall measurements of superlattices with increasing LuAs deposition per period. (a) Dark resistivity of superlattices increases with LuAs deposition. Superlattices grown with bismuth and a slow LuAs growth rate exhibited higher resistivities than other superlattices except at the 1.6 ML depositions where the resistivities seem to converge then separate due to the decreasing structural quality of the InGaAs matrix that employed only the surfactant enhancement. The dashed line represents the resistivity of epitaxial (UID) InGaAs. (b) Electron mobility decreases with increasing LuAs deposition. Superlattices that combined bismuth and a slow 0.01 ML/s LuAs growth rate lessened the rate of decline and exhibited uniformly higher mobilities than all other superlattices.

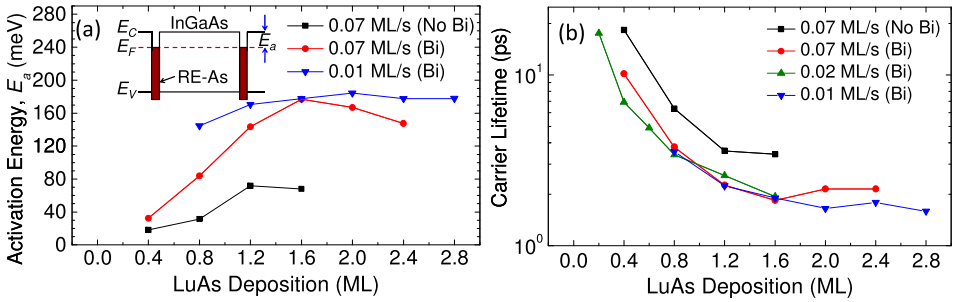

FIG. 3. (a) Activation energy of LuAs:InGaAs superlattices with increasing LuAs deposition per period. The superlattices that combined bismuth and slow 0.01 ML/s LuAs growth rate exhibited the highest activation energy of 185 meV. The inset figure shows a nearly flatband band diagram (1-D Poisson) for one superlattice period using an activation energy of 185 meV as the Schottky barrier height and the carrier concentration from room temperature Hall as the doping level for the InGaAs. (b) Carrier lifetime, measured by differential pump-probe transmission, of superlattices with increasing deposition of LuAs per period. Overall trends in the carrier lifetime seem more affected by the presence of bismuth during growth than by the LuAs growth rate. Superlattices using bismuth and a 0.01 ML/s LuAs growth rate achieved the lowest carrier lifetimes at 1.6 ps for a depositions of 2.8 ML per period.

fraction of the nanoparticle/matrix interfacial area being comprised primarily of (001) planes; in essence, the larger-sized nanoparticles begin to approach the limit of a planar (001) Schottky barrier between InGaAs and LuAs films. Introducing other crystallographic planes at the nanoparticle/matrix interface decreases the activation energy and moves the average Fermi level closer to the InGaAs conduction band edge,[26] due to the reduced Schottky barrier height of these vicinal heterointerfaces.[62,63] Therefore, the activation energy is expected to decrease as the nanoparticle/matrix interface degrades with higher depositions of LuAs. This effect is evident in the red curve of Fig. 3(a) (0.07 ML/s with bismuth) for LuAs depositions >1.6 ML and is consistent with the degradation observed with AFM and HR-XRD shown in Fig. 1(a).

Charge carrier lifetimes, shown in Fig. 3(b), were measured by time-resolved differential pump-probe transmission at 1550 nm following the methods reported earlier.[37,64] The superlattices with the combined growth enhancements reached a minimum measured carrier lifetime of 1.6 ps for the 2.8 ML deposition, a modest improvement from the 1.8 ps exhibited by the 1.6 ML superlattice with bismuth surfactant alone. Although the decrease in the carrier lifetime can be attributed to the improved structural quality of the InGaAs matrix by the bismuth, the nanoparticle morphology changes resulting from the lower LuAs growth rate seem to have very little effect on the carrier lifetime at depositions of ≤1.6 ML. Because the combined enhancements delay the structural degradation of the overgrowth to higher depositions, the defect densities that scatter the charge carriers and increase the carrier lifetime likely remained lower with the combined enhancements, assuming a diffusion limited process[64,65] for this relatively large superlattice period, as compared with the surfactant-mediated growth alone. The change in the number of defect densities is not expected to affect the carrier lifetime directly as they do not have density of states required to influence the main recombination mechanism and instead act as scatterers that prevent carriers from reaching the nanoparticles. Hence, the carrier lifetime continued to decrease for superlattices with ≥2.0 ML LuAs depositions that use the combined enhancements and explains the moderate divergence in the lifetime trends for high-growth rate LuAs depositions exceeding 1.6 ML.

In summary, the structural material quality, electrical properties, and carrier lifetimes of superlattices of LuAs embedded in an InGaAs matrix were investigated under conditions that combined the use of bismuth surfactant during the InGaAs growth and lower LuAs growth rates. The combination of bismuth as a surfactant during InGaAs overgrowth and decreased RE-As growth rate have enabled significant improvements in the key properties crucial for THz photoconductive devices. Structural quality improved significantly at elevated LuAs depositions, enabling ~50% increase in the amount of RE-As deposited before the InGaAs degraded, when compared to the control superlattices. The electrical properties also improved, with dark resistance increasing up to ~25×, while maintaining mobilities >3000 cm^2/V-s even at the highest LuAs depositions studied. The activation energies were higher for the structures with the combined enhancements over the

bismuth enhancement alone, reaching a maximum of 185 meV. Carrier lifetimes also showed a modest improvement of ~11%, achieving a lifetime as low as 1.6 ps for a 2.8 ML LuAs deposition superlattice, despite the rather large 40 nm superlattice period. Future studies should (1) apply these enhancements to shorter period superlattices to yield <1 ps lifetimes and (2) introduce antimony and/or dilute amounts of bismuth[24] into the InGaAs matrix to further improve the dark resistivity and lifetime.

This work was supported by Army Research Office through the PECASE program (No. W911NF-09-1-0434). The authors thank Professors Yaguo Wang and Wenzhi Wu from the University of Texas at Austin Department of Mechanical Engineering.

[1] J. F. Federici, B. Schulkin, F. Huang, D. Gary, R. Barat, F. Oliveira, and D. Zimdars, Semicond. Sci. Technol. **20**, S266 (2005).
[2] P. H. Siegel, IEEE Trans. Microwave Theory Tech. **50**, 910 (2002).
[3] M. Tonouchi, Nat. Photonics **1**, 97 (2007).
[4] A. Y. Pawar, D. D. Sonawane, K. B. Erande, and D. V. Derle, Drug Invent. Today **5**, 157 (2013).
[5] S. K. Mathanker, P. R. Weckler, and N. Wang, Trans. ASABE **56**, 1213 (2013).
[6] R. Kohler, A. Tredicucci, F. Beltram, H. E. Beere, E. H. Linfield, A. G. Davies, D. A. Ritchie, R. C. Iotti, and F. Rossi, Nature **417**, 156 (2002).
[7] M. A. Belkin, F. Capasso, F. Xie, A. Belyanin, M. Fischer, A. Wittmann, and J. Faist, Appl. Phys. Lett. **92**, 201101 (2008).
[8] K. Vijayraghavan, Y. Jiang, M. Jang, A. Jiang, K. Choutagunta, A. Vizbaras, F. Demmerle, G. Boehm, M. C. Amman, and M. A. Belkin, Nat. Commun. **4**, 2021 (2013).
[9] S. Jung, A. Jiang, Y. Jiang, K. Vijayraghavan, X. Wang, M. Troccoli, and M. A. Belkin, Nat. Commun. **5**, 4267 (2014).
[10] A. Maestrini, I. Mehdi, J. Siles, J. Ward, R. Lin, B. Thomas, C. Lee, J. Gill, G. Chattopadhyay, E. Schlecht, J. Pearson, and P. Siegel, IEEE Trans. Terahertz Sci. Technol. **2**, 177 (2012).
[11] H. Kanaya, H. Shibayama, R. Sogabe, S. Suzuki, and M. Asada, Appl. Phys. Express **5**, 124101 (2012).
[12] E. R. Brown, K. A. McIntosh, F. W. Smith, M. J. Manfra, and C. L. Dennis, Appl. Phys. Lett. **62**, 1206 (1993).
[13] E. R. Brown, Int. J. High Speed Electron. Syst. **13**, 497 (2003).
[14] K. A. McIntosh, E. R. Brown, K. B. Nichols, O. B. McMahon, W. F. DiNatale, and T. M. Lyszczarz, Appl. Phys. Lett. **67**, 3844 (1995).
[15] I. S. Gregory, C. Baker, W. R. Tribe, I. V. Bradley, M. J. Evans, E. H. Linfield, A. G. Davies, and M. Missous, IEEE J. Quantum Electron. **41**, 717 (2005).
[16] E. R. Brown, Appl. Phys. Lett. **75**, 769 (1999).
[17] A. W. Jackson, Ph.D. dissertation (University of California Santa Barbara, 1999).
[18] C. Kadow, Ph.D. dissertation (University of California Santa Barbara, 2000).
[19] J. E. Bjarnason, T. L. J. Chan, A. W. M. Lee, E. R. Brown, D. C. Driscoll, M. Hanson, A. C. Gossard, and R. E. Muller, Appl. Phys. Lett. **85**, 3983 (2004).
[20] J. F. O'Hara, J. M. O. Zide, A. C. Gossard, A. J. Taylor, and R. D. Averitt, Appl. Phys. Lett. **88**, 251119 (2006).
[21] E. M. Krivoy, H. P. Nair, A. M. Crook, S. Rahimi, S. J. Maddox, R. Salas, D. A. Ferrer, V. D. Dasika, D. Akinwande, and S. R. Bank, Appl. Phys. Lett. **101**, 141910 (2012).
[22] N. T. Yardimci, R. Salas, E. M. Krivoy, H. P. Nair, S. R. Bank, and M. Jarrahi, Opt. Express **23**, 32035 (2015).
[23] S. H. Yang, R. Salas, E. M. Krivoy, H. P. Nair, S. R. Bank, and M. Jarrahi, J. Infrared, Millimeter, Terahertz Waves **37**, 640 (2016).
[24] C. C. Bomberger, J. Nieto-Pescador, M. R. Lewis, B. E. Tew, Y. Wang, D. B. Chase, L. Gundlach, and J. M. O. Zide, Appl. Phys. Lett. **109**, 172103 (2016).
[25] E. R. Brown, D. C. Driscoll, and A. C. Gossard, Semicond. Sci. Technol. **20**, S199 (2005).
[26] D. C. Driscoll, Ph.D. dissertation (University of California Santa Barbara, 2004).
[27] G. H. Dohler, F. Renner, O. Klar, M. Eckardt, A. Schwanhauber, S. Malzer, D. Driscoll, M. Hanson, A. C. Gossard, G. Loata, T. Loffler, and H. Roskos, Semicond. Sci. Technol. **20**, S178 (2005).
[28] S. Preu, F. H. Renner, S. Malzer, G. H. Dohler, L. J. Wang, M. Hanson, A. C. Gossard, T. L. J. Wilkinson, and E. R. Brown, Appl. Phys. Lett. **90**, 212115 (2007).
[29] T. Ishibashi, N. Shimizu, S. Kodama, H. Ito, T. Nagatsuma, and T. Furuta, in Ultrafast Electronics and Optoelectronics, 1997, UC3, available at http://www.opticsinfobase.org/abstract.cfm?URI=UEO-1997-UC3.
[30] E. Rouvalis, C. C. Renaud, D. G. Moodie, M. J. Robertson, and A. J. Seeds, Opt. Express **18**, 11105 (2010).
[31] C. W. Berry, M. R. Hashemi, S. Preu, H. Lu, A. C. Gossard, and M. Jarrahi, Appl. Phys. Lett. **105**, 011121 (2014).
[32] C. W. Berry, M. R. Hashemi, S. Preu, H. Lu, A. C. Gossard, and M. Jarrahi, Opt. Lett. **39**, 4522 (2014).
[33] C. Baker, I. S. Gregory, W. R. Tribe, I. V. Bradley, M. J. Evans, E. H. Linfield, and M. Missous, Appl. Phys. Lett. **85**, 4965 (2004).
[34] R. J. B. Dietz, B. Globisch, M. Gerhard, A. Velauthapillai, D. Stanze, H. Roehle, M. Koch, T. Gobel, and M. Schell, Appl. Phys. Lett. **103**, 061103 (2013).
[35] D. C. Driscoll, M. Hanson, C. Kadow, and A. C. Gossard, Appl. Phys. Lett. **78**, 1703 (2001).
[36] M. Sukhotin, E. R. Brown, A. C. Gossard, D. Driscoll, M. Hanson, P. Maker, and R. Muller, Appl. Phys. Lett. **82**, 3116 (2003).
[37] R. Salas, S. Guchhait, S. D. Sifferman, K. M. McNicholas, V. D. Dasika, E. M. Krivoy, D. Jung, M. L. Lee, and S. R. Bank, Appl. Phys. Lett. **106**, 081103 (2015).

[38] J. M. Zide, D. O. Klenov, S. Stemmer, A. C. Gossard, G. Zeng, J. E. Bowers, D. Vashaee, and A. Shakouri, Appl. Phys. Lett. **87**, 112102 (2005).
[39] L. E. Clinger, G. Pernot, T. E. Buehl, P. G. Burke, A. C. Gossard, C. J. Palmstrom, A. Shakouri, and J. M. O. Zide, J. Appl. Phys. **111**, 094312 (2012).
[40] C. C. Bomberger, L. R. Vanderhoef, A. Rahman, D. Shah, D. B. Chase, A. J. Taylor, A. K. Azad, M. F. Doty, and J. M. O. Zide, Appl. Phys. Lett. **107**, 102103 (2015).
[41] C. Kadow, J. A. Johnson, K. Kolstad, and A. C. Gossard, J. Vac. Sci. Technol., B: Nanotechnol. Microelectron.: Mater., Process., Meas., Phenom. **21**, 29 (2003).
[42] M. P. Hanson, Ph.D. dissertation (University of California Santa Barbara, 2007).
[43] M. P. Hanson, D. C. Driscoll, J. D. Zimmerman, A. C. Gossard, and E. R. Brown, Appl. Phys. Lett. **85**, 3110 (2004).
[44] R. Salas, S. Guchhait, K. M. McNicholas, S. D. Sifferman, V. D. Dasika, D. Jung, E. M. Krivoy, M. L. Lee, and S. R. Bank, Appl. Phys. Lett. **108**, 182102 (2016).
[45] S. D. Sifferman, H. P. Nair, R. Salas, N. T. Sheehan, S. J. Maddox, A. M. Crook, and S. R. Bank, IEEE J. Sel. Top. Quantum Electron. **21**, 1 (2015).
[46] G. Feng, K. Oe, and M. Yoshimoto, J. Cryst. Growth **301–302**, 121 (2007).
[47] E. Young, S. Tixier, and T. Tiedje, J. Cryst. Growth **279**, 316 (2005).
[48] X. Lu, D. Beaton, R. Lewis, T. Tiedje, and M. Whitwick, Appl. Phys. Lett. **92**, 192110 (2008).
[49] C. Colinet, J. Alloys Compd. **225**, 409 (1995).
[50] A. P. Bayanov, Russ. Chem. Rev. **44**, 122 (1975).
[51] R. Hanks and M. M. Faktor, Trans. Faraday Soc. **63**, 1130 (1967).
[52] Y. Zhang, K. G. Eyink, J. Peoples, K. Mahalingam, M. Hill, and L. Grazulis, J. Cryst. Growth **435**, 62 (2016).
[53] B. D. Schultz and C. J. Palmstrøm, Phys. Rev. B: Condens. Matter Mater. Phys. **73**, 241407(R) (2006).
[54] B. D. Schultz, S. G. Choi, and C. J. Palmstrom, Appl. Phys. Lett. **88**, 243117 (2006).
[55] J. K. Kawasaki, R. Timm, T. E. Buehl, E. Lundgren, A. Mikkelsen, A. C. Gossard, and C. J. Palmstrøm, J. Vac. Sci. Technol., B: Nanotechnol. Microelectron.: Mater., Process., Meas., Phenom. **29**, 03C104 (2011).
[56] D. C. Driscoll, M. P. Hanson, E. Mueller, and A. C. Gossard, J. Cryst. Growth **251**, 243 (2003).
[57] C. Kadow, J. A. Johnson, K. Kolstad, J. P. Ibbetson, and A. C. Gossard, J. Vac. Sci. Technol., B: Nanotechnol. Microelectron.: Mater., Process., Meas., Phenom. **18**, 2197 (2000).
[58] T. Sands, C. Palmstrom, J. Harbison, V. Keramidas, N. Tabatabaie, T. Cheeks, R. Ramesh, and Y. Silberberg, Mater. Sci. Rep. **5**, 99 (1990).
[59] C. J. Palmstrom, Annu. Rev. Mater. Sci. **25**, 389 (1995).
[60] D. O. Klenov, D. C. Driscoll, A. C. Gossard, and S. Stemmer, Appl. Phys. Lett. **86**, 111912 (2005).
[61] D. O. Klenov, J. M. Zide, J. D. Zimmerman, A. C. Gossard, and S. Stemmer, Appl. Phys. Lett. **86**, 241901 (2005).
[62] C. J. Palmstrom, T. L. Cheeks, H. L. Gilchrist, J. G. Zhu, C. B. Carter, B. J. Wilkens, and R. Martin, J. Vac. Sci. Technol., A **10**, 1946 (1992).
[63] K. T. Delaney, N. A. Spaldin, and C. G. Van de Walle, Phys. Rev. B: Condens. Matter Mater. Phys. **81**, 165312 (2010).
[64] D. C. Driscoll, M. P. Hanson, A. C. Gossard, and E. R. Brown, Appl. Phys. Lett. **86**, 051908 (2005).
[65] C. Kadow, S. B. Fleischer, J. P. Ibbetson, J. E. Bowers, A. C. Gossard, J. W. Dong, and C. J. Palmstrom, Appl. Phys. Lett. **75**, 3548 (1999).